Particle transport in density gradient driven TE mode turbulence

A. Skyman[1], H. Nordman[1], P. I. Strand[1]

[1]Euratom–VR Association, Department of Earth and Space Sciences,
Chalmers University of Technology, SE-412 96 Göteborg, Sweden

Abstract

The turbulent transport of main ion and trace impurities in a tokamak device in the presence of steep electron density gradients has been studied. The parameters are chosen for trapped electron (TE) mode turbulence, driven primarily by steep electron density gradients relevant to H-mode physics. Results obtained through non-linear (NL) and quasilinear (QL) gyrokinetic simulations using the GENE code are compared with results obtained from a fluid model. Impurity transport is studied by examining the balance of convective and diffusive transport, as quantified by the density gradient corresponding to zero particle flux (impurity peaking factor). Scalings are obtained for the impurity peaking with the background electron density gradient and the impurity charge number. It is shown that the impurity peaking factor is weakly dependent on impurity charge and significantly smaller than the driving electron density gradient.

1 Introduction

The compatibility between a reactor-grade plasma and the material walls surrounding the plasma is one of the main challenges facing a magnetic fusion device. The presence of very low levels of high Z impurities in the core plasma may lead to unacceptable levels of radiation losses and fuel dilution. Also low Z impurities, in the form of beryllium or helium-ash, may result in fuel dilution that severely limits the attainable fusion power [1]. Consequently, the transport properties of impurities is a high priority issue in present experimental and theoretical fusion plasma research. This is emphasised by the the new ITER-like wall experiment in JET [2], where a beryllium-clad first wall in the main chamber, combined with carbon and tungsten tiles in the divertor, will be tested for the first time.

The transport of main fuel as well as impurities in the core region of tokamaks is expected to be dominated by turbulence driven by Ion Temperature Gradient (ITG) modes and Trapped Electron (TE) modes. The main drives for the ITG/TE mode instabilities are gradients of temperature and density combined with unfavourable magnetic curvature. Most of the theoretical studies of turbulent particle transport have been devoted to temperature gradient driven ITG and TE modes, using both fluid, and quasilinear (QL) and nonlinear (NL) gyrokinetic models [3–24]. Much less effort has been devoted to particle transport in regions with steep density gradients. The density gradient, which is stabilising for ITG modes, provides a drive for TE modes which may dominate the temperature gradient drive for plasma profiles with $R/L_{n_e} > R/L_{T_e}$. This may occur in connection with the formation of transport barriers, like the high confinement mode (H-mode) edge pedestal, in fusion plasmas.

In the present article, the turbulent transport of main ion and trace impurities in tokamaks is investigated through nonlinear (NL) gyrokinetic simulations using the GENE code.[1] The main part considers collisionless TE modes driven by density gradients. The impurity density gradient for zero impurity flux is calculated for varying background electron density gradient drive and for a range of impurity species. This study complements recent studies [23, 24] on temperature gradient driven TE and ITG mode impurity transport. The NL GENE results are compared with QL gyrokinetic simulations and a computationally efficient multi fluid model, suitable for use in predictive transport simulations. Of particular interest is the sign of the impurity convective flux and the degree of impurity peaking in the presence of strong background electron density gradients.

The remainder of the article is structured as follows: in section 2 impurity transport is briefly reviewed, with emphasis on topics relevant to the study; this is followed by section 3 on the simulations and a discussion of the main results. The article concludes with section 4, containing a summary of the main conclusions to be drawn.

2 Transport models

The models used have been described in detail elsewhere, see [23] and references therein, only a brief summary is given here.

The NL and QL GENE simulations were performed in a flux tube geometry, in a low β ($\beta = 10^{-4}$) s–α equilibrium [25–28]. The simulations include gyrokinetic electrons (passing and trapped), and gyrokinetic main ions and impurities. Effects of finite β, plasma shaping, equilibrium $\boldsymbol{E} \times \boldsymbol{B}$ flow shear and collisions have been neglected. The effects of collisions are known to be important for the turbulent fluctuation and transport levels [29], however, their effects on the impurity peaking factor have been shown to be small [12]. In order to ensure that the resolution was adequate, the resolution was varied separately for the perpendicular, parallel and velocity space coordinates, and the effects of this on the mode structure, $k_\perp$ spectra and flux levels were investigated. The resolution was then set sufficiently high for the effects on these indicators to have converged. For a typical NL simulation for main ions, fully kinetic electrons, and one trace species, a resolution of $n_x \times n_y \times n_z = 96 \times 96 \times 24$ grid points in real space and of $n_v \times n_\mu = 48 \times 12$ in velocity space was chosen. For QL GENE simulations the box size was set to $n_x \times n_y \times n_z = 8 \times 1 \times 24$ and $n_v \times n_\mu = 64 \times 12$ respectively. The impurities were included self-consistently as a third species in the simulations, with the trace impurity particle density $n_Z/n_e = 10^{-6}$ in order to ensure that they have a negligible effect on the turbulence.

For the fluid simulations, the Weiland multi-fluid model [30] is used to derive the main ion, impurity, and trapped electron density response from the corresponding fluid equations in the collisionless and electrostatic limit. The fluid simulations include first order Finite Larmor-Radius (FLR) effects for the main ions, and parallel main ion/impurity dynamics. The free electrons are assumed to be Boltzmann distributed. The equations are closed by the assumption of quasineutrality.

An eigenvalue equation for TE, ITG and ETG modes is thus obtained in the presence of impurities. A strongly ballooning eigenfunction with $k_\parallel^2 = \left(3q^2R^2\right)^{-1}$ valid for magnetic shear $s \sim 1$ is used [31]. The eigenvalue equation is then reduced to a system of algebraic equations that is solved numerically.

---

[1] http://www.ipp.mpg.de/~fsj/gene/

The main ion and impurity particle fluxes can then be written as:

$$\Gamma_j = \langle \delta n_j v_E \rangle = -n_j \rho_s c_s \left\langle \widetilde{n}_j \frac{1}{r} \frac{\partial \widetilde{\phi}}{\partial \theta} \right\rangle . \tag{1}$$

Here v_E is the radial $\boldsymbol{E} \times \boldsymbol{B}$ drift velocity, $\rho_s = c_s/\Omega_{ci}$ is ion sound scale, with $c_s = \sqrt{T_e/m_i}$ being the ion sound speed and $\Omega_{ci} = eB/m$ the ion cyclotron frequency. On the right hand side, the perturbations in density and electrostatic potential are defined $\widetilde{n}_j = \delta n_j/n_j$ and $\widetilde{\phi} = e\phi/T_e$ respectively. The angled brackets in equation (2) imply a time and space average over all unstable modes. Performing this averaging, the particle flux can be written:

$$\frac{R\Gamma_j}{n_j} = D_j \frac{R}{L_{n_j}} + D_{T_j} \frac{R}{L_{T_j}} + RV_{p,j}. \tag{2}$$

The first term in equation (3) corresponds to diffusion, the second to the thermodiffusion and the third to the convective velocity (pinch), where $1/L_{n_j} = -\nabla n_j/n_j$, n_j is the density of species j and R is the major radius of the tokamak. The pinch contains contributions from curvature and parallel compression effects. The terms of equation (3) have been described in detail in previous work [17–19, 23]. For trace impurities, equation (3) can be uniquely written

$$\frac{R\Gamma_Z}{n_Z} = D_Z \frac{R}{L_{n_Z}} + RV_Z, \tag{3}$$

where D_Z is the impurity diffusion coefficient and V_Z is the total impurity convective velocity with the thermodiffusive term included, and neither D_Z nor V_Z depend on $1/L_{n_Z}$. The sign of the thermodiffusive, or "thermopinch", term is decided mainly by the real frequency, $\widetilde{\omega}_r$. For electron modes $\widetilde{\omega}_r = R\omega_r/c_s < 0$, resulting in the thermodiffusion generally giving an inward contribution to the pinch for TE modes. For an impurity with charge number Z, this term scales as $D_{T_Z} \sim (1/Z)(R/L_{T_Z})$ to leading order, rendering it unimportant for large Z impurity species, but it is important for lighter elements, such as the He ash.

The zero-flux impurity density gradient (peaking factor) is defined as $PF_Z = -RV_Z/D_Z$ for the value of the impurity density gradient that gives zero impurity flux. The peaking factor thus quantifies the balance between convective and diffusive impurity transport. Solving the linearised equation (4) for R/L_{n_Z} with $\Gamma_Z = 0$ yields the interpretation of PF_Z as the gradient of zero impurity flux. It is found by first computing the impurity particle flux Γ_Z for values of R/L_{n_Z} in the vicinity of $\Gamma_Z = 0$. The diffusivity (D_Z) and convective velocity (V_Z) are then given by fitting the acquired fluxes to equation (4), whereafter the peaking factor is obtained through their quotient. This is illustrated in figure 1.

3   Simulation results

The main parameters used in the simulations are summarised in table 1. The parameters where chosen to represent an arbitrary tokamak geometry at about mid radius, and do not represent any one particular experiment. A moderately steep electron temperature gradient ($R/L_{T_e} = 5.0$) together with a flatter ion temperature gradient ($R/L_{T_i,Z} = 2.0$) was used to promote TE mode dominated dynamics. Following [32], the background density gradient for the base scenario was set higher than the temperature gradient, to ensure density gradient driven dynamics. In order to preserve quasineutrality $\nabla n_e = \nabla n_i$ was used. The quasilinear gyrokinetic and fluid results were calculated for a single poloidal mode number with $k_\theta \rho_s = 0.2$; see [23] for a discussion on the choice of $k_\theta \rho_s$.

First, the main ion particle flux (Γ_p) is studied. Time averaged fluxes are calculated from time series of NL GENE data after convergence, as illustrated in figure 2a. The scalings of Γ_p with the electron density gradient obtained from NL GENE and fluid simulations are shown in figure 2b. The fluid and nonlinear gyrokinetic model show similar scalings for the main ion flux, but the gyrokinetic transport exhibits a stronger dependence on R/L_{n_e}. This is in line with the trends seen for the linear eigenvalues, as show in figure 2c. The NL GENE and fluid results presented in figure 2b indicate that for the present parameters, neither model gives a main ion flux reversal for TE mode driven turbulence.

Next, the scaling of the impurity transport with the background density gradient (R/L_{n_e}) is investigated. The results for the impurity peaking factor are shown in figure 3a. We note that the impurity peaking increases with R/L_{n_e}, saturating at $PF_Z \approx 2.0$ for large values of the electron density gradient. The QL GENE results tend to consistently overestimate the peaking factors compared to the NL GENE results, while the fluid model gives results that are somewhat below the NL GENE results for the steeper gradients. The fluid results show a considerably less dramatic dependency of the peaking factor than the QL and NL gyrokinetic results, both of which show a strong decrease in PF_Z as the electron density profiles flatten. This is observed for all values of the impurity charge number. As the background density profile becomes more peaked, a corresponding increase in impurity transport is expected. This is illustrated in figure 3b, where scalings, obtained from NL GENE simulations, of the diffusivity (D_Z) and convective velocity (RV_Z) with R/L_{n_e} are shown. Although the magnitudes of D_Z and RV_Z both show a strong increase with R/L_{n_e}, in accordance with the scaling of the growth rate seen in figure 2c, the impurity peaking ($PF_Z = -RV_Z/D_Z$) is only weakly sensitive to the electron density gradient. For $R/L_{n_e} \lesssim 2.0$ the impurity peaking factor is not well defined, since both D_Z and RV_Z go to zero. The fluid and gyrokinetic results are in qualitative agreement, showing a growth rate that increases uniformly with R/L_{n_e}. For the studied parameters, there are no clear signs of a transition from density gradient driven to temperature gradient driven TE mode turbulence, which has been reported to dominate for $R/L_{n_e} \lesssim R/L_{T_e}$ [32].

The scaling of the impurity peaking factor with impurity charge (Z), with R/L_{n_e} as a parameter, is illustrated in figure 4. The impurity charge was varied from $Z = 2$ (He) to $Z = 42$ (Mo). The models show only a very weak scaling, with PF_Z falling toward saturation for higher Z. The results are similar to those for the temperature gradient driven TE mode reported in [24]. Notably, the QL GENE simulations overestimate the peaking factors compared to the NL GENE results, whereas the fluid results are lower than the NL GENE results. The scalings observed for low Z impurities ($Z \lesssim 10$) is weak or reversed compared to results for the ITG mode driven case, reported in e.g. [23], where a strong rise in PF_Z with increasing Z was obtained. The qualitative difference between the TE and the ITG mode dominated cases can be understood from the Z-dependent thermodiffusion in equation (3), which is outward for ITG modes and inward for TE modes.

4   Conclusions

In summary, the turbulent transport of main ion and trace impurities in regions of steep density gradients has been investigated through nonlinear (NL) gyrokinetic simulations using the GENE code. The simulations included gyrokinetic electrons (passing and trapped), and gyrokinetic main ions and impurities in a low β s–α equilibrium. The main part has considered collisionless TE modes driven by steep density gradients, a parameter regime of relevance for the formation of transport barriers in fusion plasmas. The NL GENE results for the density gradient of zero impurity particle flux (peaking factor) have been compared with QL kinetic simulations and a

reduced and computationally efficient multi-fluid model, suitable for use in predictive transport simulations. In the simulations, the magnetic shear and safety factor were held fixed at $s = 0.8$ and $q = 1.4$. For the parameters studied, qualitative agreement between gyrokinetic and fluid results has been obtained for the scaling of the impurity peaking factor with both the background density gradient and the impurity charge. An inward impurity convective velocity, corresponding to positive peaking factor, was found in all cases considered. In the region of steep electron density gradients, it was shown that the impurity peaking factor saturates at values significantly smaller than the driving electron density gradient. In general, a good qualitative agreement between the considered models was found. It was, however, noted that for the chosen length scales ($k_\theta \rho_s = 0.2$), the QL GENE, in comparison with the NL GENE results, tended to overestimate the peaking factors, whereas the fluid results were close to or lower than the NL GENE results. The scaling of the peaking factor with impurity charge was observed to be weak, with a slight increase in the impurity peaking factor observed in the gyrokinetic results for low impurity charge numbers.

Acknowledgements

References

[1] Harte C S, Suzuki C, Kato T, Sakaue H A, Kato D, Tamura N, Sudo S, D'Arcy R, Sokell E, White J and O'Sullivan G 2010 *J. Phys. B* **43** 205004

[2] Matthews G F, Edwards P, Greuner H, Loving A, Maier H, Martens P, Philipps V, Riccardo V, Rubel M, Ruset C, Scmidt A and Villedieu E 2009 *Phys. Scr.* **2009** 014030

[3] Fröjdh M, Liljeström M and Nordman H 1992 *Nucl. Fusion* **32** 419

[4] Basu R, Jessen T, Naulin V and Rasmussen J J 2003 *Phys. Plasmas* **10** 2696

[5] Estrada-Mila C, Candy J and Waltz R 2005 *Phys. Plasmas* **12** 022305

[6] Naulin V 2005 *Phys. Rev. E* **71** 015402

[7] Priego M, Garcia O E, Naulin V and Rasmussen J J 2005 *Phys. Plasmas* **12** 062312

[8] Fülöp T and Weiland J 2006 *Phys. Plasmas* **13** 112504

[9] Bourdelle C, Garbet X, Imbeaux F, Casati A, Dubuit N, Guirlet R and Parisot T 2007 *Phys. Plasmas* **14** 112501

[10] Dubuit N, Garbet X, Parisot T, Guirlet R and Bourdelle C 2007 *Phys. Plasmas* **14** 042301

[11] Camenen Y, Peeters A G, Angioni C, Casson F J, Hornsby W A, Snodin A P and Strintzi D 2009 *Phys. Plasmas* **16** 012503

---

[12] Fülöp T, Braun S and Pusztai I 2010 *Phys. Plasmas* **17** 062501

[13] Futatani S, Garbet X, Benkadda S and Dubuit N 2010 *Phys. Rev. Lett.* **104** 015003

[14] Hein T and Angioni C 2010 *Phys. Plasmas* **17** 012307

[15] Moradi S, Tokar M Z and Weyssow B 2010 *Phys. Plasmas* **17** 012101

[16] Fülöp T and Moradi S 2011 *Phys. Plasmas* **18** 030703

[17] Nordman H, Singh R, Fülöp T, Eriksson L G, Dumont R, Andersson J, Kaw P, Strand P, Tokar M and Weiland J 2008 *Phys. Plasmas* **15** 042316

[18] Angioni C and Peeters A G 2006 *Phys. Rev. Lett.* **96** 095003

[19] Nordman H, Fülöp T, Candy J, Strand P and Weiland J 2007 *Phys. Plasmas* **14** 052303

[20] Angioni C, Carraro L, Dannert T, Dubuit N, Dux R, Fuchs C, Garbet X, Garzotti L, Giroud C, Guirlet R, Jenko F, Kardaun O J W F, Lauro-Taroni L, Mantica P, Maslov M, Naulin V, Neu R, Peeters A G, Pereverzev G, Puiatti M E, Pütterich T, Stober J, Valovič M, Valisa M, Weisen H, Zablotsky A, ASDEX Upgrade team and JET–EFDA contributors 2007 *Phys. Plasmas* **14** 055905

[21] Angioni C, Peeters A G, Pereverzev G V, Bottino A, Candy J, Dux R, Fable E, Hein T and Waltz R E 2009 *Nucl. Fusion* **49** 055013

[22] Fülöp T and Nordman H 2009 *Phys. Plasmas* **16** 032306

[23] Nordman H, Skyman A, Strand P, Giroud C, Jenko F, Merz F, Naulin V, Tala T and the JET–EFDA contributors 2011 *Plasma Phys. Contr. F.* **53** 105005

[24] Skyman A, Nordman H and Strand P 2012 Impurity transport in temperature gradient driven turbulence to be published in Phys. Plasmas URL `arXiv:1107.0880`

[25] Jenko F, Dorland W, Kotschenreuther M and Rogers B N 2000 *Phys. Plasmas* **7** 1904

[26] Dannert T 2005 *Gyrokinetische Simulation von Plasmaturbulenz mit gefangenen Teilchen und elektromagnetischen Effekten* Ph.d. thesis Technischen Universität München

[27] Dannert T and Jenko F 2005 *Phys. Plasmas* **12** 072309

[28] Merz F 2008 *Gyrokinetic Simulation of Multimode Plasma Turbulence* Ph.d. thesis Westfälischen Wilhelms-Universität Münster

[29] Angioni C, Candy J, Fable E, Maslov M, Peeters A G, Waltz R E and Weisen H 2009 *Phys. Plasmas* **16** 060702

[30] Weiland J 2000 *Collective Modes in Inhomogeneous Plasmas* (IoP Publishing)

[31] Hirose A, Zhang L and Elia E 1994 *Phys. Rev. Lett.* **72** 3993–3996

[32] Ernst D R, Lang J, Nevins W M, Hoffman M and Chen Y 2009 *Phys. Plasmas* **16** 055906

Table 1: Parameters used in the fluid and gyrokinetic simulations, [†] denotes scan parameters

|	R/L_{n_e}-scaling:	Z-scaling:
T_i/T_e:	1.0	1.0
s:	0.8	0.8
q:	1.4	1.4
β:	10^{-4}	10^{-4}
$\varepsilon = r/R$:	0.14	0.14
$k_\theta \rho_s$:	0.2	0.2
$n_e,\, n_i + Z\, n_Z$:	1.0	1.0
n_Z (trace):	10^{-6}	10^{-6}
$R/L_{T_i},\, R/L_{T_Z}$:	2.0	2.0
R/L_{T_e}:	5.0	5.0
$R/L_{n_{i,e}}$:[†]	1.0–13.0	5.0–13.0
Z:[†]	2, 28	2–42
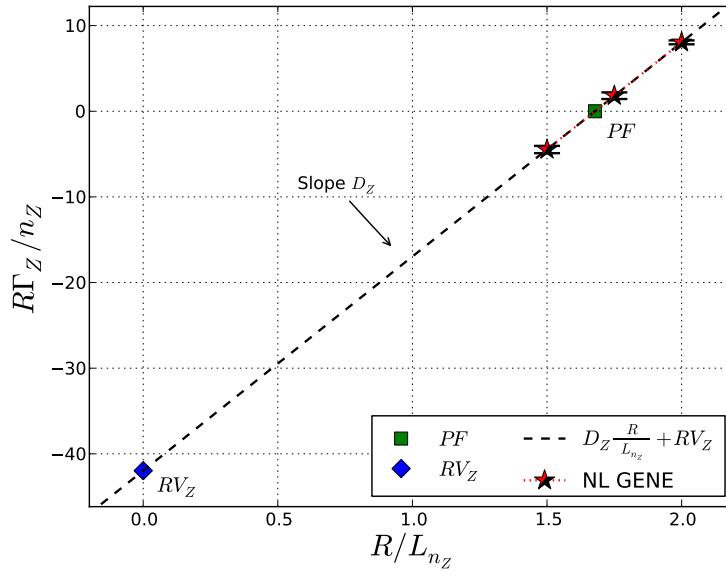
Figure 1: Impurity flux (Γ_Z) as a function of the impurity density gradient ($-R\nabla n_Z/n_Z = R/L_{n_Z}$), illustrating the process of finding the impurity peaking factor (PF_Z), diffusivity (D_Z) and convective velocity (V_Z). NL GENE data of TEM turbulence in a proton plasma with He impurities, and background density gradient $R/L_{n_e} = 5.0$.
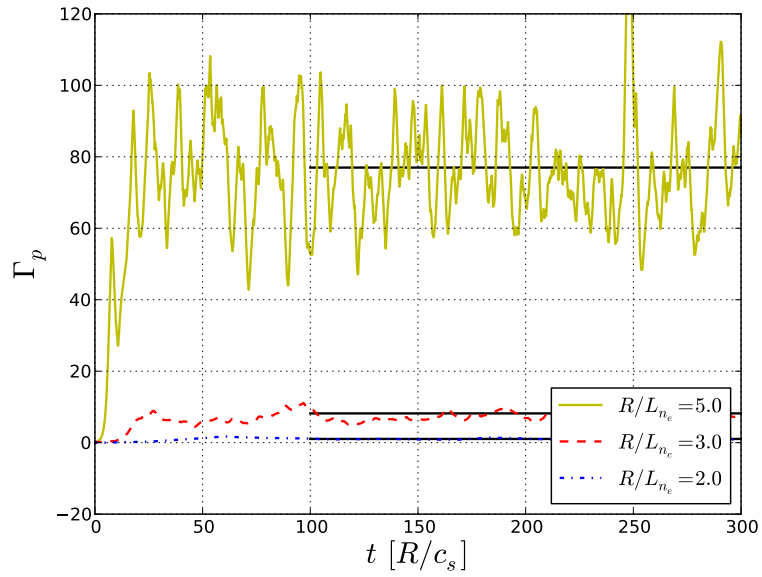
(a) time series and time averages of the main ion flux (Γ_p) from NL GENE simulations

(b) main ion flux (Γ_p) dependence on the background density gradient (R/L_{n_e}).

9
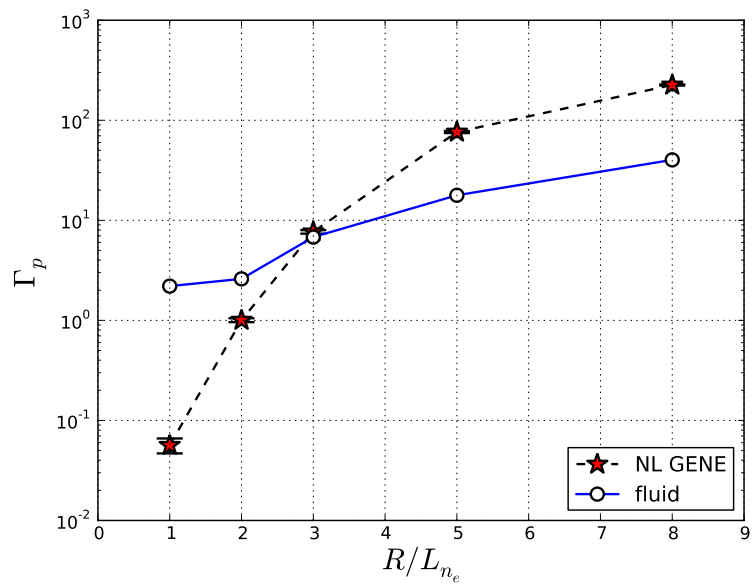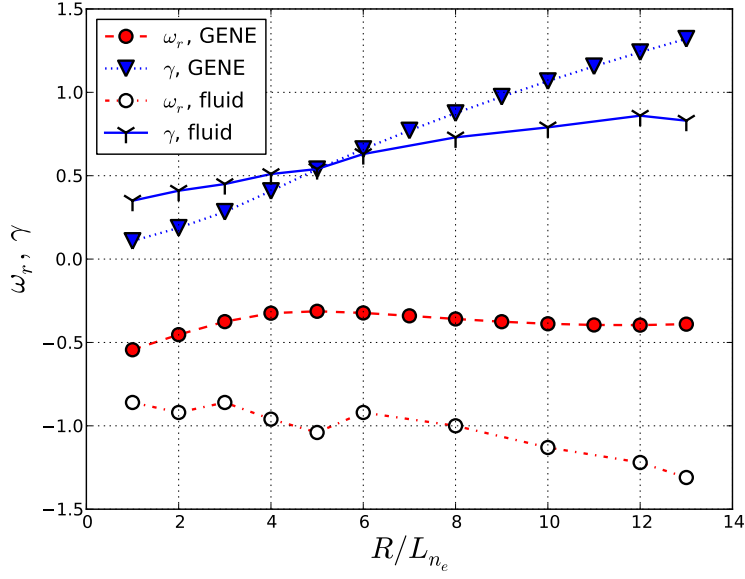
(c) scaling of real frequency (ω_r) and growth rate (γ) with the background density gradient

Figure 2: Main ion flux (Γ_p) dependence on the background electron density gradient ($-R\nabla n_e/n_e = R/L_{n_e}$). NL GENE and fluid data with protons as main ions. Parameters are $q = 1.4$, $s = 0.8$, $\varepsilon = r/R = 0.14$, $R/L_{T_i,Z} = 2.0$, $R/L_{T_e} = 5.0$, and $\tau = T_e/T_i = 1.0$. The fluid data was obtained for $k_\theta \rho_s = 0.2$. The fluxes are normalised to $v_{T,i} n_e \rho_i^2/R^2$. The error bars indicate an estimated uncertainty of one standard deviation. The eigenvalues in figure 2c are from fluid and GENE simulations, and are normalised to c_s/R.
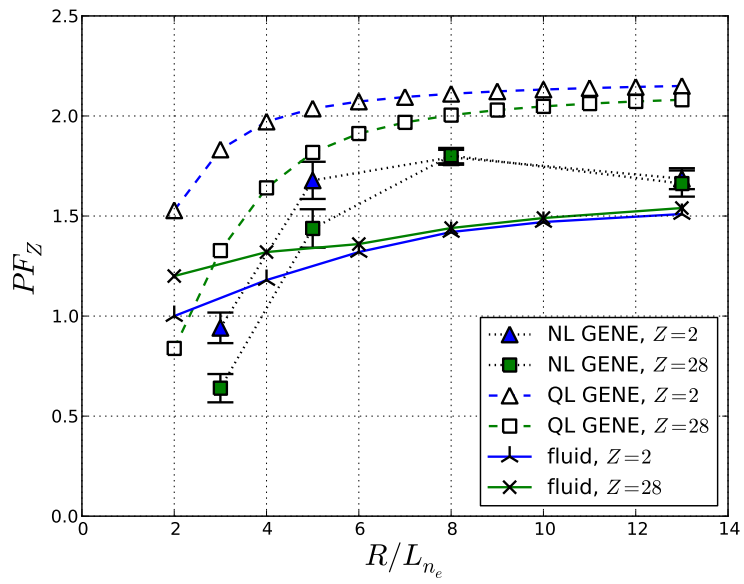
(a) dependence of the impurity peaking factor (PF_Z) on the background density gradient
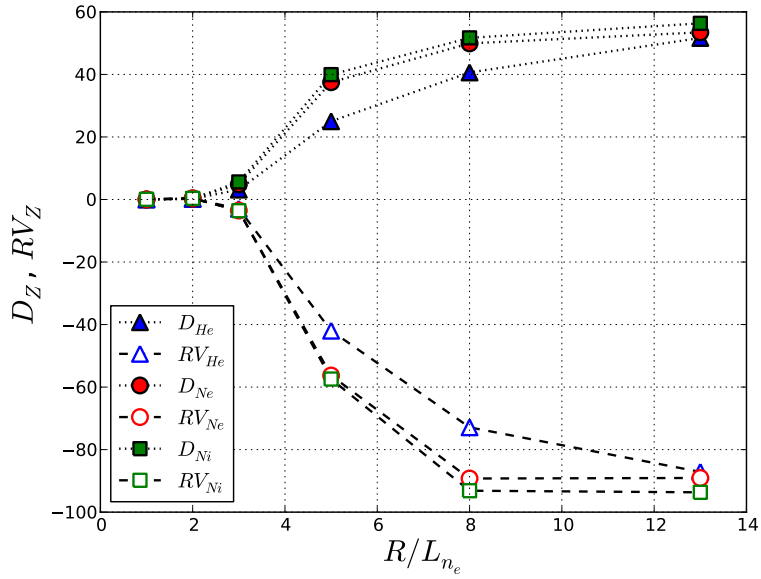
(b) dependence of the impurity diffusivity and convective velocity (D_Z and RV_Z) on the background density gradient

Figure 3: Scalings of the impurity peaking factor ($PF_Z = -RV_Z/D_Z$) with the background electron density gradient (R/L_{n_e}), with parameters as in figure 2. QL and fluid data have been acquired using $k_\theta \rho_s = 0.2$. Figure 3b shows the diffusivities and pinches corresponding to the NL GENE impurity peaking factors (PF_Z) in figure 3a. D_Z and RV_Z are normalised to $v_{T,i}\rho_i^2/R$. The error bars indicate an estimated uncertainty of one standard deviation.
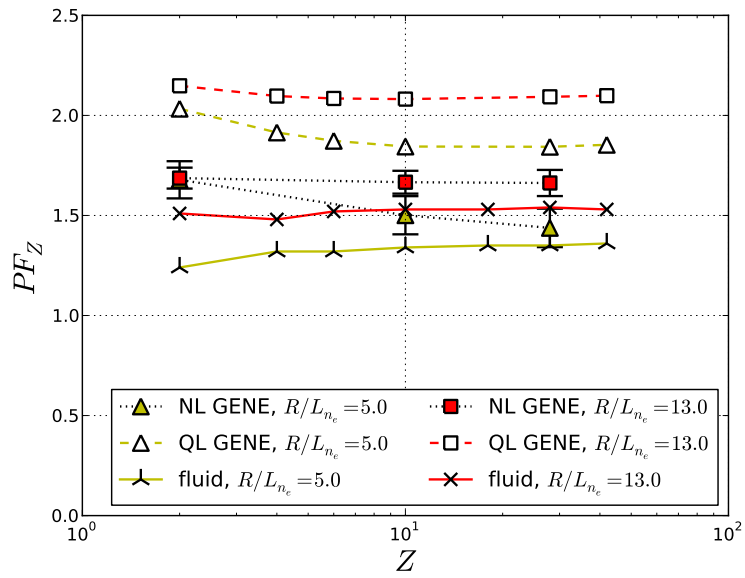
Figure 4: Scaling of the impurity peaking factor ($PF_Z = -RV_Z/D_Z$) with impurity charge Z, with parameters as in figure 2; $k_\theta \rho_s = 0.2$ was used in the QL and fluid simulations. The error bars indicate an estimated uncertainty of one standard deviation.